

# Chapter 5

## 3D Topological Scanning and Multi-material Additive Manufacturing for Facial Prosthesis Development



Mazher I. Mohammed, Joseph Tatineni, Brenton Cadd, Greg Peart, and Ian Gibson

### 5.1 Introduction

In a human population, facial defects can arise as a result of congenital deformities, disease infiltration, and trauma. Given the prominence of the face and how it influences human interactions, such disfigurements can have a profoundly negative impact on quality of life, often requiring repeated surgical interventions that aim on improving aesthetic appeal. With respect to rehabilitation, there are primarily two treatment options comprising either surgical intervention or the use of a prosthesis. The decision-making process over which option is the most suitable is not so clearly defined and dependent on a number of factors, ranging across the size/severity of the condition, age and aetiology as well as the patient's own personal preference [1, 2]. When considering prosthesis-based rehabilitation, there are several immediate advantages when compared with surgical intervention such as the immediate aesthetic improvement, its simplicity over surgery and consequently the reduced risk to the patient, the ability to explore numerous design iterations without impacting the patient and its comparatively low cost. More recently, there has been a surge of interest in tissue engineering approaches to replace missing or compromised organs [3, 4]. Despite the obvious potential of this technology, there are still many issues to resolve before this is likely to become a mainstream approach. Therefore, prosthetic

---

M. I. Mohammed · J. Tatineni  
School of Engineering, Deakin University, Geelong, VIC, Australia  
e-mail: [mazher.m@deakin.edu.au](mailto:mazher.m@deakin.edu.au); [dawn.joseph@deakin.edu.au](mailto:dawn.joseph@deakin.edu.au)

B. Cadd · G. Peart  
Facial Prosthetics, The Royal Melbourne Hospital, Parkville, VIC, Australia  
e-mail: [brenton.cadd@mh.org.au](mailto:brenton.cadd@mh.org.au); [greg.peart@mh.org.au](mailto:greg.peart@mh.org.au)

I. Gibson (✉)  
Department of Design, Production & Management, University of Twente,  
Enschede, The Netherlands  
e-mail: [i.gibson@utwente.nl](mailto:i.gibson@utwente.nl)

treatments provide a more robust, tried and tested approach which has a relatively quick and predictable turnaround time for part production, does not require extensive follow-up treatments and generally does not result in complications that are often associated with surgical interventions, such as tissue rejection.

Despite the advantages over surgery, traditional prosthesis production is still considered to be an unacceptably long and labour-intensive process, requiring the use of numerous invasive and subjective techniques throughout the fabrication process. A summary of the general fabrication stages can be found in Fig. 5.1. Typically the process begins with some form of casting using plaster to ascertain the topology of the defective area or of uncompromised anatomy that could be used as a template for the prosthesis [5, 6]. In some instances, plaster can be placed over the entirety of a patient's face, requiring breathing to be performed through a straw until the plaster sets. Additionally, due to the discomfort of this process, the patient may move during the casting, resulting in a subjective topological map. Following the formation of the plaster cast, a wax model is formed and manipulated to create the finished prosthesis model. At this stage, fixation point alignments may also be performed, which are embedded into the wax model. The alignment and finishing of the wax model are all performed manually, with the end result being wholly dependent on the art skill and artistic interpretation of the technician and is arguably very subjective in nature [7]. Once the wax model is finalised, it is further formed into a plaster negative, which in turn is used to generate the final silicone prosthesis. Any additional touches to the model, such as the addition of colours and hair, are again performed manually at this stage. It is clear to see that this whole process of prosthesis production is extremely arduous and labour intensive.

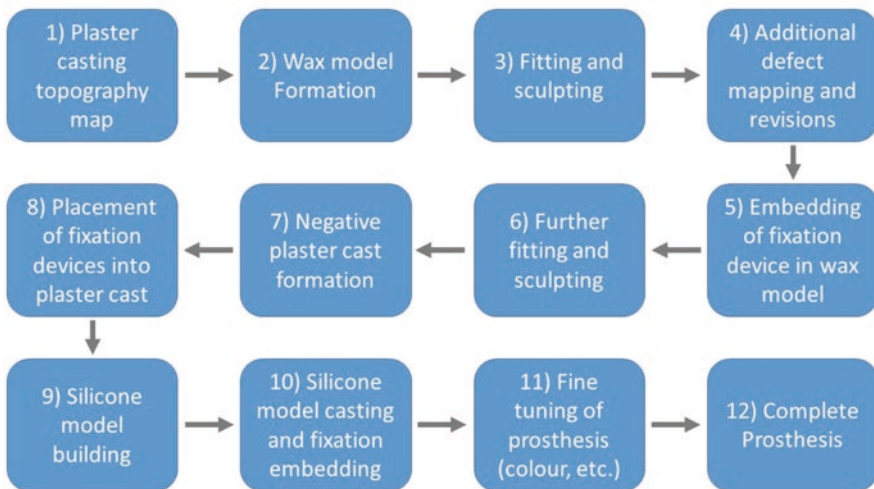


**Fig. 5.1** Traditional process chain for external prosthesis fabrication

Traditional prosthesis development appears to be approaching a turning point, where several disruptive 3D technologies are likely to transform the previously mentioned process. Modern optical scanning technologies are now readily available and allow for the rapid, high-resolution reproduction of surface topologies to a precision of  $<100\ \mu\text{m}$  whilst capturing useful data such as the texture of a patient's skin [8–10]. Additionally, such data is obtained non-invasively and can even be performed using laser-free methodologies that greatly improve the potential uptake in a clinical setting. Modern computer-aided design (CAD) software can readily manipulate this 3D scan data to create a complete model, with the added advantage of digitally recording the design iterations and storing the final model so that it may be used multiple times and in different contexts. Such digital data capture and storage, when applied to prosthesis production, compares very favourably to traditional hand-crafting techniques. Furthermore, modern additive manufacturing (AM, also referred to as 3D printing) technologies offer the ability to easily and rapidly reproduce the high-resolution digital model into a physical part [10–16]. Fabrication in this manner could be achieved using flexible and biocompatible materials, allowing for augmentation of existing practises and potentially could be applied to direct prosthesis fabrication.

In this study, we have investigated the use of optical scanning, reverse engineering, CAD and additive manufacturing towards the direct production of various facial prostheses (ear and nose). Previous studies have focused on the use of such technologies for the production of castings to augment traditional techniques or for parts made in rigid plastics. By contrast, the novelty in this work is the use of high-resolution AM with graded flexible material capability for the direct production of a prosthesis which not only results in a higher-quality surface finish, compared with the previous studies, but also mimics the tactile feel and pigmentation of human soft tissue. We also investigate the production of advanced prosthetic models, comprising multi-material designs, which more closely reproduce human tissue through mimicry of both the skin and cartilage. Our technique offers several advantages over traditional approaches such as the use of optical scanning for topological mapping. This approach is non-invasive, can acquire data within minutes and realises anatomically precise, high-resolution data sets that are ideal for prosthesis production. A digital CAD approach for prosthesis design is superior when compared with traditional casting and handcrafting because design iterations can be easily digitally stored, do not require any fabrication/material consumption and allow for operations such as mirroring of the original data set. Finally, the use of high-precision additive manufacturing allows for rapid digital part realisation and can produce a sophisticated prosthesis that comprises complex multi-material structures and can further allow for precise reproduction should duplicates be required. Ultimately, we believe the techniques presented in this work can realise a patient specific, low-cost and high-resolution approach to streamlining prosthesis optimisation and production.

## 5.2 Experimental

In this study, we have investigated the use of several 3D digitising, rendering and printing technologies to directly create prosthesis replica from a person's anatomy. The complete process chain can be seen in Fig. 5.2, where surface topology maps are made using an optical scanner, designs are post-processed using reverse engineering software followed by CAD and the final model is realised using high-resolution, multi-material AM.

### 5.2.1 Topology Mapping and Model Construction

In this study, a laser-free, optical scanning system (Spider, Artec, Luxembourg) was employed to obtain the surface topology of the nose and ear of a volunteer subject. Laser-free scanning technology alleviated any health concerns resulting from laser exposure to the eyes. The scanner used had an image scan resolution of approximately 50–100  $\mu\text{m}$ , which is more than adequate to resolve all the major and minor details of the anatomical part rendered. The scanner operated alongside a proprietary software (Artec Studio 10, Artec, Luxembourg), which allows for the real-time visualisation of the scan data during acquisition. It was found that several translations of the scanner were required to obtain the full surface map, comprising movements at approximately 10 cm/s in a lateral and vertical arcing motion. The scanner allowed for the regions of interest to be captured and rendered rapidly within approximately 3–5 minutes.

The scanner software processes the input data as a point cloud, which is then converted into a full contour map by simply joining these points together using adjacent vectors. Rudimentary operations can be performed within the Artec software to condition the data, remove spurious noise, crop unrequired data regions, fill

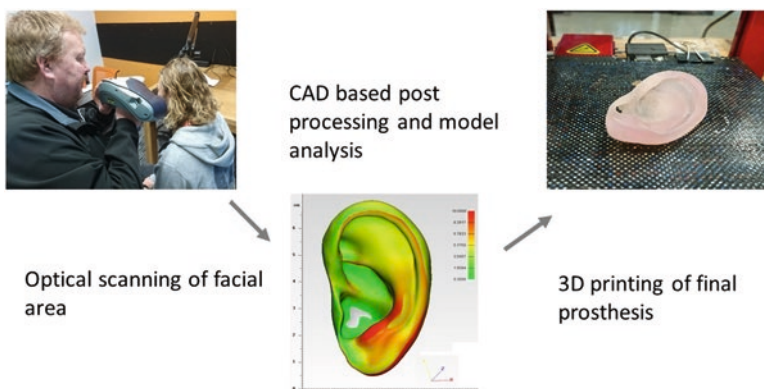


Fig. 5.2 Diagram illustrating the proposed process chain for prosthesis production

holes/gaps in the model and smooth contours. The resulting model appears in a form that is a completely enclosed model exported in the industry standard STL file format for AM. However, further post-processing may be required to the hollow part for the purposes of lightweighting, for example, and realise features such as nasal cavities and ear canals. Such features may correlate to regions where the scanner cannot cover due to overshadowing of other features, for example. In most cases, it would not be appropriate to push or pull on the patient to enable the scanning process as the intention would be to capture the surfaces in their natural state. This may be particularly problematic around the back of the ear, for example, although it should normally be fine to pin back the hair of the subject.

### ***5.2.2 Model Construction and Post-processing***

Data from the scanner was further conditioned using more sophisticated CAD software to process the surface topological data and to construct more advanced models for composite model printing. In this study, all additional post-processing was performed using the 3-Matic software package (Materialise, Belgium), which can allow for direct STL data manipulation, error checking and geometric measurements such as part thickness analysis. Data conditioning in our approach comprised smoothing of apparently rough surfaces, removing features that could lead to failure of the model when printing and performing procedures such as part hollowing. The need to smoothen rough surfaces is a particularly subjective decision. It may be that the surfaces are slightly corrupted by reflective artefacts. It may also be that the scanned surfaces are in fact rough due to scar tissue or other blemishes. The degree and regions for smoothing would therefore be a clinical decision.

Some of the scanning techniques had previously been developed in conjunction with the facial prosthetics group at the Royal Melbourne Hospital [17]. This study used AM to create a pattern based on scan data which was then manually manipulated to create a final silicone part for the patient. The major benefits of this approach lay in the speed and convenience of the scanning plus the accuracy of the pattern. In this further study, we aimed to realise an advanced prosthesis using AM that closely mimics human physiology in terms of tactile feel and pigmentation. As a demonstrator, we took a constructed model of the ear using the scanning approach earlier described. We then manipulated it to build separate models of the cartilage and a composite of the softer tissues. The regions representing the cartilage model were constructed using purely a design-based approach, selecting the regions within the data set using tools in 3-Matic. To obtain anatomical accuracy, the model was constructed by cross-referencing anatomical drawings of the ear cartilage and correlating that with qualitative measurements from direct feel of the test subject's actual ear. Approximations were then used to determine the layer thickness of the skin relative to the cartilage in the model. Once this was done, the remaining data inside the skin was considered to be cartilage. These two model sets can then be referenced to different material (i.e. stiffness) properties.

### 5.2.3 *Additive Manufacturing*

Once rendering and post-processing had been completed, the final models were directly 3D printed to produce the final prosthesis. To obtain acceptable accuracy in digital reproduction, a high-resolution AM machine (printer) was used (Connex 3, Stratasys, USA) which can print models in up to three individual materials or blends thereof to an accuracy of 16  $\mu\text{m}$  layer thickness and 30  $\mu\text{m}$  in-plane resolution. This was considered to be more than adequate for the reproduction of all major and minor surface contours. It also realises a sufficiently high-quality surface finish for the prosthesis, similar to that obtained by traditional manual techniques.

Using AM machines such as the Connex 3, a model is loaded into the printer's software as an STL file and then allocated specific process parameters before being sliced into the individual layers for printing. Simultaneously, a water-soluble support material is automatically generated at this stage of the process and allocated to ensure the build integrity. The printer operates using PolyJet™ technology, whereby liquid photo-curable polymers are delivered in droplet form by a printhead and subsequently flattened and cured by a UV lamp. Once a build has been completed, a subsequent cleaning phase is required to remove the surrounding support material before the part is ready for use. The printing process can take on average 2–3 hours for a part the size of an ear or nose to be printed, depending the orientation and whether there are other parts being built at the same time.

The printer used in this study was capable of printing in several different materials, which have a variety of colours and mechanical properties. For instance, the Tango Plus™ material range is a flexible monochrome material, whilst Vero™ materials are rigid and coloured. For the final prosthesis parts, we examined a combination of both Tango plus and Vero materials such that we could obtain a final model with not only a compliant tactile feel but also with adjustable colours. It was our hope in this study to realise combinations that mimic the feel and pigmentation of a person's actual tissue. Further, the advanced multi-model approach allows for further control of the tactile feel of a given anatomical part.

## 5.3 Results

### 5.3.1 *Scanning and Model Creation*

Various scans were performed on a test subject in an attempt to reproduce the surface topology of their nose and left ear. In this instance, the subject was a healthy individual who suffered no significant injury or facial defects. This allowed for a relatively simple comparison of the printed prosthesis with the original anatomy. When performing scans, the Fast Fusion™ mode of the scanner was utilised, which allowed for rapid, real-time visualisation of the scans on the computer as they were being performed. Scans were carried out by translating the scanner

through the various orientations previously described. Following completion of the data acquisition, several additional data conditioning phases were performed using Artec Studio to remove obvious unwanted regions and spurious noise and to reconstruct small gaps in the data. Following completion of the scans, the software allowed for several automated procedures to merge multiple scans together, crop the part of interest from the wider facial data and convert the scan from a surface to a fully enclosed mesh.

It was found that there were limitations to the scanning process, and areas of the skin which were shiny/reflective were difficult to render during scanning. This limitation could be overcome using a matt powder to dampen optical reflections. Additionally, regions which had low levels of light exposure or shadowing were equally difficult to render, such as the nasal cavities, behind the ear and the ear canal. As such features are critical to the final prosthesis, they had to be rendered independently using the 3-Matic software.

### **5.3.2 Model Post-processing**

#### **5.3.2.1 Single Model**

Following initial rendering, the models were checked using the Artec software to remove errors such as inverted normal vectors, multiple shells, noisy shells, among others. This procedure ensures the best-quality digital data for the subsequent design phases. Qualitatively, the rendered models from the scanner looked reasonably close to the original anatomy and the final prosthesis models that were printed, and so in this case, only relatively simple post-processing was required. With respect to the nose data, the nasal cavities were completely enclosed, and so the first procedure was to remove excess digital material to open these areas and to provide access to the reverse side of the model. The necessity for this is that a recipient of such a prosthesis may still have use of their nasal ducts, and so open access here would allow for a potential patient to retain the ability to breathe, smell, etc. With respect to the ear data, by cross referencing the major contours against the original test subject, it was found that several of the contours formed by the cartilage had been lost during the post-processing using the Artec Software. These areas were subsequently manually reconstructed using the 'push/pull' and 'extrude' functions within 3-Matic. Figure 5.3a illustrates the final model of the ear prosthesis.

With respect to the ear, when a thickness analysis was performed, it was found that there were regions which were  $<350\ \mu\text{m}$  thick. Whilst this may not be an issue to the aesthetics within the digital mode, should this be printed, these regions would be extremely fragile. Initial test prints with this thickness in the rubber, such as Tango Plus material, found that they ruptured during the support material removal phase. Several design iterations were examined, increasing the minimum thickness in steps of approximately  $200\ \mu\text{m}$ . It was found that with thicknesses

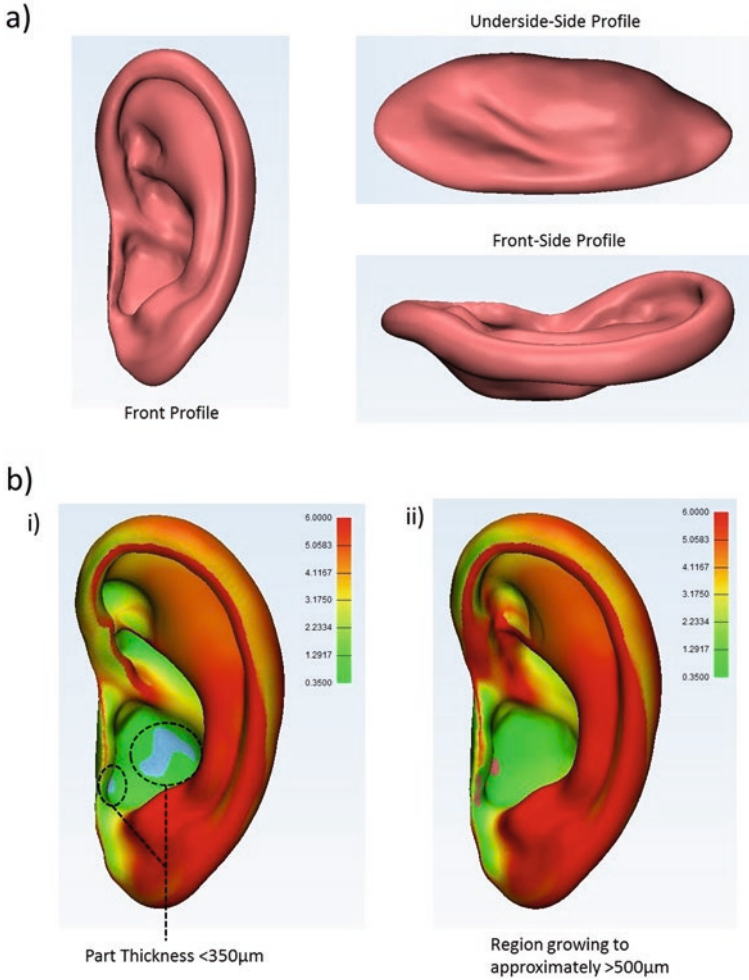


**Fig. 5.3** (a) Various orientations of the ear prosthesis model. (b) Colour map thickness analysis of the ear model for (i) the raw data model input from the 3D scanner software and (ii) post-processed model to grow the thickness of the inner ear section to  $\geq 1$  mm

greater than 1 mm, the models could be cleaned without rupturing. Therefore, a thickness analysis of the part to be built is critical to the integrity of the final prosthesis using the Tango Plus material, and parts should be thoroughly inspected to ensure no regions exist with a thickness less than 1 mm. Figure 5.3b shows a model of the ear before and after the thickness analysis and subsequent model region growing.



### 5.3.2.2 Multicomponent Ear Modelling

The anatomy of the human ear comprises a single piece of skin-covered cartilage tissue in the ear which makes the design process relatively simple in comparison with more complex cartilage structures in organs such as the nose. Initially attempts were made to render the cartilage of the ear as a stand-alone model. To achieve this, the original ear model was duplicated and reduced in size by 96% to create a replica structure that was positioned approximately 1.5 mm into the original ear model. This new model was then reformed with reference to anatomical drawings of a generic human ear cartilage, the contours of the scanned ear model and by direct feel of the original human subject. Despite being a subjective metric for development of a design, the feel of the subject's ear provided valuable insight into the patient-specific anatomy of the ear, whilst the anatomical medical diagrams provided a framework for the general shape of the ear. The final model that was achieved can be seen in Fig. 5.4, which closely matched the medical diagrams.

### 5.3.3 Prosthesis Fabrication Using Additive Manufacturing

#### 5.3.3.1 Single Model Printing

Following completion of the models, initial tests were performed to ascertain the printing precision, model integrity, mechanical conformity and pigmentations that could be achieved using a multi-material combinatory approach. The Connex printer is capable of printing with three materials simultaneously; however, as flexibility

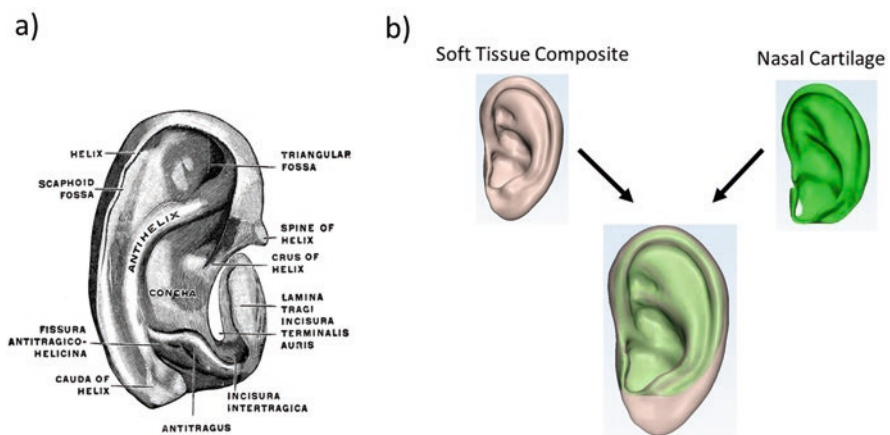


**Fig. 5.4** (a) A classical medical diagram of the cartilage within the ear [18]. (Adapted from [https://lookfordiagnosis.com/mesh\\_info.php?term=ear+cartilage&lang=1](https://lookfordiagnosis.com/mesh_info.php?term=ear+cartilage&lang=1)). (b) The multi-model design of the ear prosthesis comprising the soft tissue composite and the cartilage. For visualisation purposes both segments are also represented individually

was desirable through the use of Tango plus, only two additional materials (colours) could be used. Given the availability of colours by the manufacturers, it was decided that blends of magenta and yellow would provide the best options for skin pigmentation mimicry. A colour map was produced using the Connex machine of the different material combinations when using Tango plus and Vero materials, which can be seen in Fig. 5.5a. Another constraint that arose was the percentage blend of the rigid Vero with the flexible Tango plus material. Values of greater than 50–60% Vero material provided a tactile feel beyond the desired flexibility found in a typical prosthesis. The Tango plus material used in this study was a translucent variant, which on its own provided the softest tactile feel but was not a suitable colour for a prosthesis. It was found that a minimum of 10% Vero material was required to provide

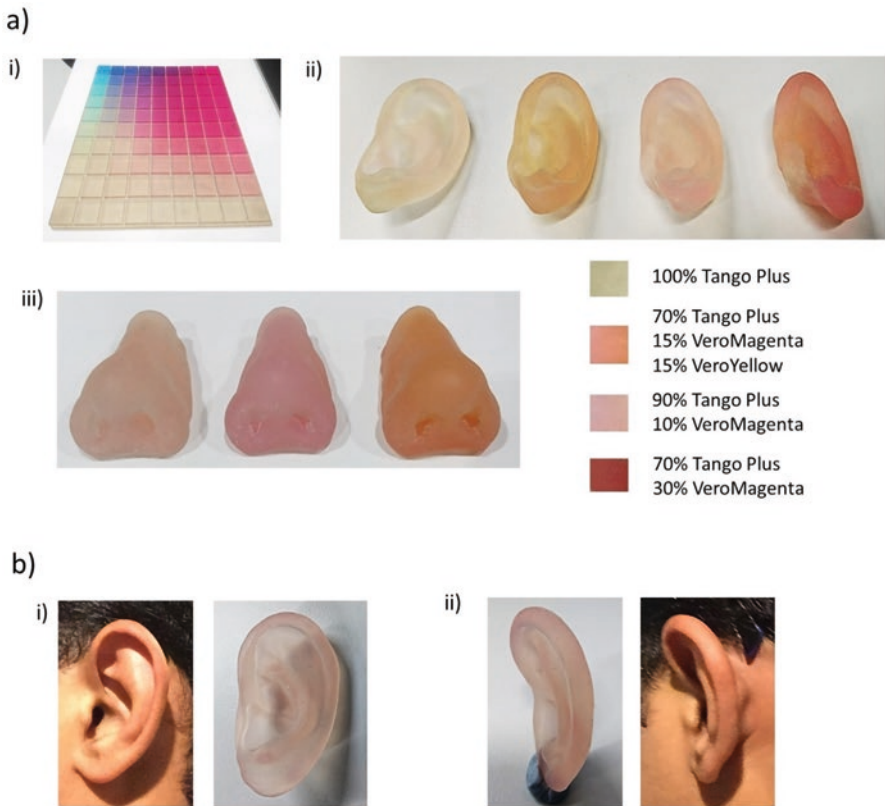


**Fig. 5.5** (a) (i) A image of the material map which shows the various colour combinations possible with the 3D printer using two Vero colours and the flexible Tango plus material and images of various printed prosthesis of (ii) an ear and (b) a nose model. Material combinations are also highlighted in the legend. (b) Comparative images of the subject's ear and the printed model from (i) side and (ii) reverse orientations

any visually noticeable pigmentation into a given prosthesis. Various combinations of Tango and Vero material were explored to print the final prosthesis, and some of these can be seen in Fig. 5.5a.

The high resolution of the Connex printer and the use of dissolvable support material allows for the reproduction of both the ear and nose models with a smooth surface finish. The reproduced models were found to be a near identical match to the original anatomy, both in terms of major surface contours and dimensional deviations. Various nose and ear models can be seen in Fig. 5.5a (iii), showing clearly how the multi-material printing allows for a diverse array of prosthesis pigmentations from lighter to darker skin tones. Also shown in Fig. 5.5b are comparative images of the printed ear prosthesis next to the volunteer subject's original ear. It can be seen that the final prosthesis very closely matches the original contours of the ear, validating the efficacy of this technique. Upon closer examination of the ear models, it was found that the richness of the visible colour changed depending upon the thickness of the material. By comparison, the nose models failed to exhibit such features. This is perhaps due to the relative thickness ranges of these models. For the ear models, most thicknesses were between 1 and 6 mm, thus exhibiting varying degrees of translucency. By contrast, the minimum thickness of the nose was approximately 15 mm. At these thicknesses, all translucency effects are negligible. This is similar to human physiology, where the thickness of the soft tissues overlaying the cartilage of the ear has a variety of different pigmentations owing to its relative thickness. We hope to examine such effects more closely in future work.

The printed models were qualitatively assessed for their tactile feel and mechanical compliance in comparison with the original human subject. Tests comprised the ability to flex the lobe area, a vertical compression test from the lobe to the upper portion of the ear and a lateral compression test pinching across the centre of the ear. It was found that the printed models all exhibited similar characteristic to the original anatomy and that upon relaxation of the compressive force, the ears would return to the neutral position, as can be seen in Fig. 5.6a. For this experiment, a range of models were created using a fixed ratio of flexible to rigid material throughout each one. It was noted that the printed material was still noticeably more rigid, despite its elasticity, than real human anatomy. This resulted in a greater force being applied to achieve the various modes of compression, highlighting limitation of current printable, flexible materials. It was also noted that as the percentage of the Vero material was increased in the model, the applied force became larger. At a percentage of 60% Vero, the elasticity of the model was compromised beyond an acceptable level and became noticeably rigid. This limits the wider colour combinations possible whilst still retaining acceptable levels of elasticity to mimic human mechanical properties. We hope in future work to quantify such forces both for real anatomy and printed prosthesis.

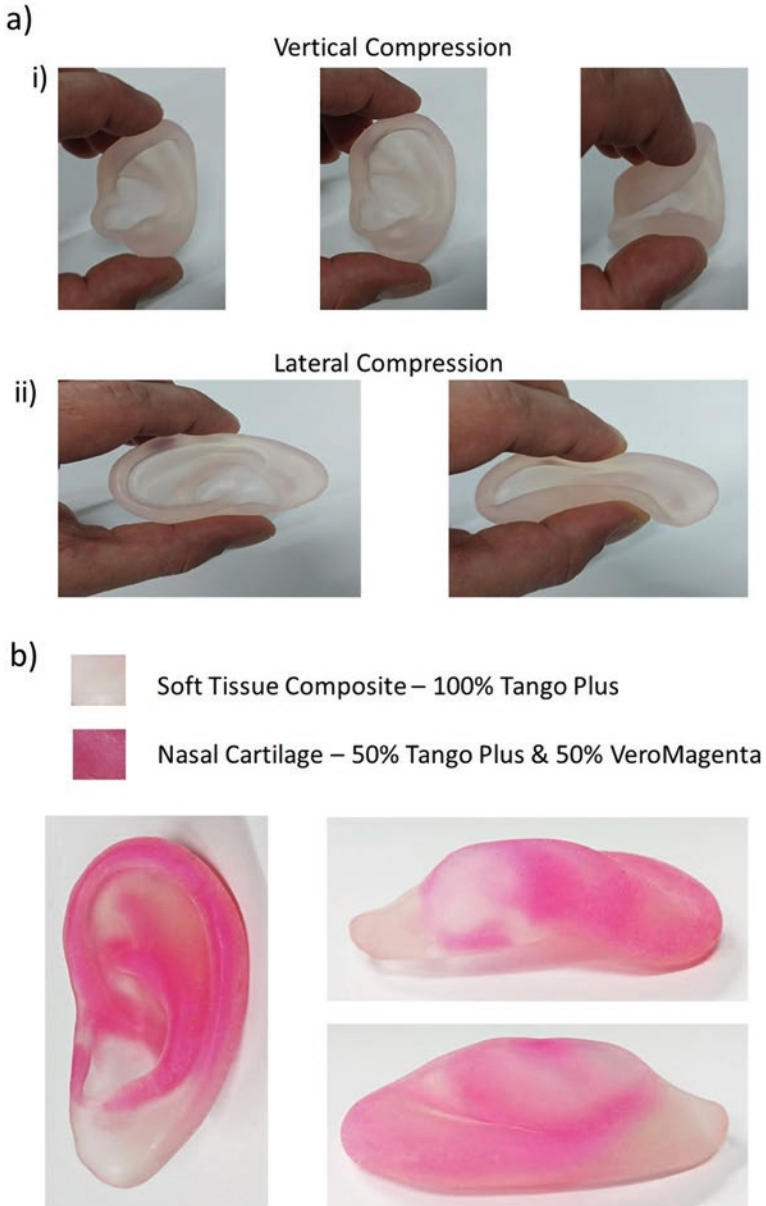


**Fig. 5.6** (a) Qualitative compression of the model to demonstrate the realism in the tactile feel for both (i) vertical and (ii) lateral compression. (b) Multi-model printing of the ear, with independent material combinations for the cartilage and residual soft tissue composite

### 5.3.3.2 Multi-model Printing

As well as the previously mentioned single material models, we attempted to realise a range of models rendered using variable material combinations throughout. The purpose of this was to more closely mimic the softer and harder tissue regions of the ear. The Connex printer allows for the nesting of multiple models and for independent material allocation to each for printing. We therefore processed the advanced ear model such that the soft tissue composite was printed with 100% Tango plus and the encapsulated cartilage model was printed with 50% Tango plus and 50% VeroMagenta. These material combinations were used primarily for visualisation purposes such that each element could be visually differentiated, and the final printed model can be seen in Fig. 5.6b. The Connex printer was found to provide excellent multi-material printability, with the two materials seamlessly blending into a single structure without any impact on the final surface finish of the model. Therefore, the PolyJet printing process of the Connex is considered ideal for rendering of not only blended materials but also multiple material models for direct prosthesis printing.

Once again, the mechanical properties of the model were assessed by qualitative compression tests. On this occasion, it was found that there was much greater rigidity to the ear model, as expected; however, the ability to be compressed vertically and laterally was not compromised, and the model would also return to the neutral position upon relaxation of the compressive force. It was noted that the movement of the ear lobe was identical to the single material/model prints. Outcomes of the multi-model printing illustrate that the mechanical properties of the printed models can be further modified to reach increasing levels of complexity, as found in actual human anatomy. We hope in the future to more quantitatively assess the mechanical properties and to explore the ability to more seamlessly blend the colour combinations into a more realistic final model.

## 5.4 Conclusions

This study has demonstrated the potential of the 3D design and multi-model/material printing, augmented with the use of optical surface scanning, to produce realistic prosthetic models of both the ear and nose. The fabricated prostheses were realised to a high degree of accuracy, and we believe the technique suitable to render additional prosthetic parts, such as for an orbital prosthesis. We realised advanced prosthesis models beyond the traditional single material variants using novel design techniques to render components such as cartilage alongside other soft tissues, such as the skin. Using the multi-material printing approach, we could tailor the skin pigmentation of the prosthesis to a variety of skin tones, whilst also mimicking the mechanical properties of the original anatomy. The mechanical properties can be further tailored using the multi-model, multi-material approach used in this study. Currently, there are limitations in the complexity of the skin tones that can be mim-

icked without compromising the mechanical properties, due to the percentage material combinations available with the machine used. Additionally, the overall printed prosthesis tactile feel is more rigid than actual anatomy. These limitations are primarily due to the materials used in the 3D printer, but we believe as the technology matures over the coming years, these limitations will be resolved. For example, this is something that the recently introduced Stratasys J750 machine should be able to overcome, since the extra printhead permits the use of all colours with the addition of material hardness variations. Ultimately, the findings in the work validate our approach for direct prosthesis production which overcome limitations relating to the subjective nature of current prosthesis fabrication and allow for production within a single day. This compares favourably to traditional techniques where typically a prosthesis is fabricated over several weeks/months. Ultimately, this technique holds considerable potential for implementation within a clinical setting, streamlining the overall process for prosthesis production and seeing applications in other niche areas such as soft robotics or anatomical modelling.

This chapter is an adaptation of a paper presented at the 27th Solid Freeform Fabrication Symposium in Austin, Texas, USA, 2017 [19].

**Acknowledgements** We would like to thank the Royal Melbourne hospital for their input on the clinical aspects of this project. We would also like to thank the School of Engineering at Deakin University who provided funds and resources for this pilot project and their technical staff who assisted in the additive manufacturing of the models.

## References

1. J.D. Kretlow, A.J. McKnight, S.A. Izaddoost, Facial soft tissue trauma. *Semin. Plast. Surg.* **24**(4), 348–356 (2010)
2. K. Ranganath, H.R. Hemant Kumar, The correction of post-traumatic pan facial residual deformity. *J. Maxillofac. Oral Surg.* **10**(1), 20–24 (2011)
3. M.S. Mannoor et al., 3D printed bionic ears. *Nano Lett.* **13**(6), 2634–2639 (2013)
4. L. Jung-Seob et al., 3D printing of composite tissue with complex shape applied to ear regeneration. *Biofabrication* **6**(2), 024103 (2014)
5. S.S. Mantri, R.U. Thombre, D. Pallavi, Prosthodontic rehabilitation of a patient with bilateral auricular deformity. *J. Adv. Prosthodont.* **3**(2), 101–105 (2011)
6. A.N. Ozturk, A. Usumez, Z. Tosun, Implant-retained auricular prosthesis: a case report. *Eur. J. Dent.* **4**(1), 71–74 (2010)
7. R.M. Jani, N.G. Schaaf, An evaluation of facial prostheses. *J. Prosthet. Dent.* **39**(5), 546–550 (1978)
8. L. Ciocca et al., CAD/CAM ear model and virtual construction of the mold. *J. Prosthet. Dent.* **98**(5), 339–343 (2007)
9. G. Sansoni et al., 3D imaging acquisition, modeling and prototyping for facial defects reconstruction. *SPIE Proc.* **7239**, 1–8 (2009)
10. D. Palousek, J. Rosicky, D. Koutny, Use of digital technologies for nasal prosthesis manufacturing. *Prosthetics Orthot. Int.* **38**, 171–175 (2014)
11. M. Al Mardini, C. Ercoli, G.N. Graser, A technique to produce a mirror-image wax pattern of an ear using rapid prototyping technology. *J. Prosthet. Dent.* **94**(2), 195–198 (2005)

12. E.J. Bos et al., Developing a parametric ear model for auricular reconstruction: a new step towards patient-specific implants. *J. Cranio-Maxillofac. Surg.* **43**(3), 390–395 (2015)
13. Y. He, G.H. Xue, J.Z. Fu, Fabrication of low cost soft tissue prostheses with the desktop 3D printer. *Sci. Rep.* **4**, 6973 (2014)
14. I. Kuru et al., A 3D-printed functioning anatomical human middle ear model. *Hear. Res.* **340**, 204–213 (2016)
15. P. Liacouras et al., Designing and manufacturing an auricular prosthesis using computed tomography, 3-dimensional photographic imaging, and additive manufacturing: a clinical report. *J. Prosthet. Dent.* **105**(2), 78–82 (2011)
16. K. Subburaj et al., Rapid development of auricular prosthesis using CAD and rapid prototyping technologies. *Int. J. Oral Maxillofac. Surg.* **36**(10), 938–943 (2007)
17. <https://www.youtube.com/watch?v=I5YthHUA9T0&t=61s>
18. [https://lookfordiagnosis.com/mesh\\_info.php?term=ear+cartilage&lang=1](https://lookfordiagnosis.com/mesh_info.php?term=ear+cartilage&lang=1)
19. M.I. Mohammed, J. Tatineni, B. Cadd, P. Peart, I. Gibson, *Applications of 3D topography scanning and multi-material additive manufacturing for facial prosthesis development and production*. Proceedings of the 27th annual international solid freeform fabrication symposium, 2016, p. 1695–1707